Pharmacological activation of antiviral ProTides

Proposed involvement of CES1 in the metabolism of Remdesivir

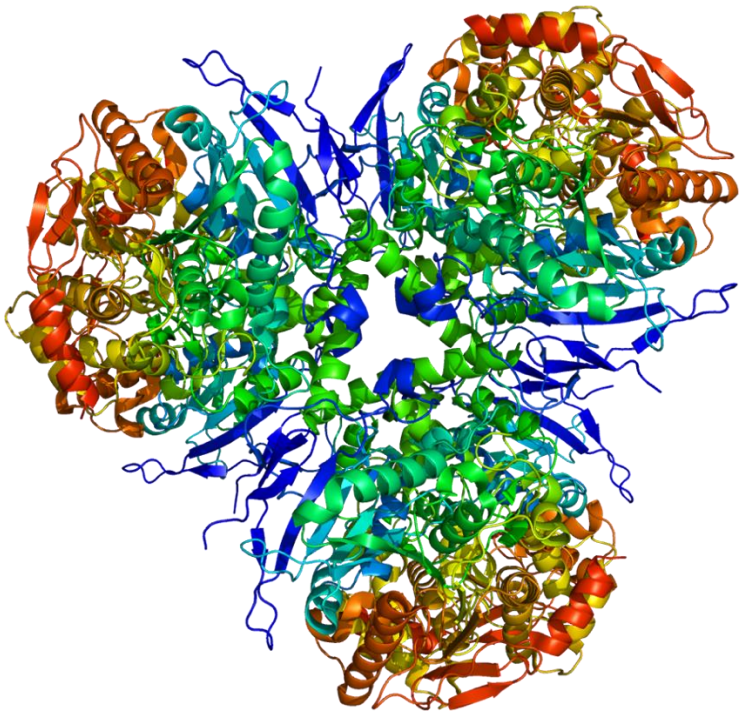

This semester project is written by:

Emira Havkic, 65186

Ilayda Dilara Pusat, 65256

Mathilde Alfang, 65235

Semester project in molecular biology 2020

NATURAL SCIENCE BACHELOR – ROSKILDE UNIVERSITY

Supervisor: Henrik Berg Rasmussen

December 18th, 2020

Preface

This project is written by students currently attending their fifth semester on the Naturel Science Bachelor program at Roskilde University.

We would like to recognize and thank our supervisor, Henrik Berg Rasmussen, who has been helpful in the making of this project. A special thanks to Kornelius Zeth for providing the components used in the laboratory and for helping plan the laboratory procedures. Finally, we would like to thank Christa Persson for assisting in the execution of the experiments.

Abstract

Prodrugs are pharmacologically inactive compounds that are metabolized in the body into an active drug. A subcategory to prodrugs is ProTides. ProTides are nucleotide analogs, meaning the drug's active metabolite has an altered nucleoside moiety and a phosphorous attachment. ProTides share a similar core structure, and the purpose of ProTides is intracellular delivery of cells infected by viruses to inhibit viral RNA elongation. Remdesivir is a ProTide, and the structural features of Remdesivir are susceptible to cleavage, hence leading to activation of the drug. It is currently unknown which enzymes are involved in the activation of the drug.

According to previously published literature, ProTides Sofosbuvir and Tenofovir undergo a series of metabolic steps to gain pharmacological activity. Carboxylesterase 1 and Cathepsin A has been proven to be responsible for the first step. This project aims to investigate whether collected information about the mentioned ProTides can be applied to propose the enzymes responsible for the initial catalyzation of Remdesivir. Based on the literature analysis, Remdesivir might be subject to hydrolyzation by CES1 and/or CatA in the first steps of activation.

Furthermore, this project contains experimental work, of which laboratory data regarding protein expression, purification, and enzyme kinetics has been collected. The former two are based on recombinant CES1 and CES2, transferred into competent E. coli cells. Enzyme kinetics was determined by spectrophotometry, and 4-nitrophenyl acetate was used as a substrate. Obtained K_m of 570 and 580 µM was similar to published literature. The laboratory work concluded successfully purified CES1 with adequate enzyme activity.

Table of content

Introduction to Problem Statement

In the light of the current coronavirus pandemic, a central point of focus is access to efficient antiviral agents to prevent further complications in infected patients (Reza Hashemian, Farhadi and Velayati, 2020) (Jovanovic *et al.*, 2020).

Previous viral epidemics and outbreaks have revealed the nucleotide analog Remdesivir as an effective treatment in patients with Ebola, MERS, and SARS (Reza Hashemian, Farhadi and Velayati, 2020). Therefore, Remdesivir is a strong antiviral candidate in the treatment of COVID-19 (Reza Hashemian, Farhadi and Velayati, 2020). Remdesivir is derived from its parent nucleoside, GS-441524 (Yan and Muller, 2020). GS-441524 has shown effective inhibition of feline infectious peritonitis, a fatal coronavirus of domestic cats (Murphy *et al.*, 2018). As the research on Remdesivir for treatment of COVID-19 is currently on-going, its metabolism, which pharmacologically activates the drug inside the human body, remains partially unknown (Jovanovic *et al.*, 2020) (Badgujar *et al.*, 2020) (Agostini *et al.*, 2018). Moreover, studies have shown that CES1, a protein highly concentrated on the endoplasmic reticula (Hosokawa, 2008), makes it a candidate for hydrolyzation in the first steps in the activation of Remdesivir. However, evidence still lacks CES1 involvement in the latter statement. Studies also suggest the enzymatic activity of Cathepsin A in the metabolism of antiviral ProTides, including Remdesivir (Yan and Muller, 2020). The enzymatic action of Remdesivir by CES1 is not well understood, and this project aims to further shed light on the possible activity of CES1 in the activation of Remdesivir.

Furthermore, this project concerns with laboratory experiments, in which CES1 expression and purification are executed. The experiments are partially a reproduction of previously completed experiments (Boonyuen *et al.*, 2015). However, minor adjustments have been applied.

Problem Statement

The problem statement is based on above introduction.

"According to published literature, which ProTides are activated by CES1, and can this support a supposed metabolism of Remdesivir? Is it possible to produces recombinant CES1 by following the methods reported in "Efficient in vitro refolding and functional characterization of recombinant human liver carboxylesterase (CES1) expressed in E. coli" by Usa Boonyuen et al. (2015)?

1.0 Introduction

The following sections describes fundamental theory and gives introduction to central components, used to answer the problem statement.

1.1 Intro to Carboxylesterase

Carboxylesterases (CES) are a family of enzymes that catalyze the hydrolysis of molecules containing ester- and amide groups. CES belongs to a super-family known as the α, β hydrolase-fold family, and are also known as serine esterases (Imai and Ohura, 2011). The different human CES enzymes are divided into at least five groups (CES1-CES5), where the prominent CES families are CES1 and CES2, which both have various CES isoenzymes (Imai and Ohura, 2011). The gene encoding CES1 is found on chromosome 16 (Bjerre and Berg Rasmussen, 2018).

CES1 are located in the endoplasmic reticulum membrane (Hosokawa, 2008), and are mainly present in the liver (Bjerre and Berg Rasmussen, 2018). Both CES1 and CES2 are involved in the metabolic activation of both drugs and prodrugs (Wang *et al.*, 2018), (Hosokawa, 2008), and CES2 are also involved in the metabolism of endogenous ester counting triacylglycerol, cholesteryl ester, and other lipids and therefore, play an essential role in the homeostasis of lipids (Wang *et al.*, 2018). CES1 and CES2 share around 47% of their amino acid sequence – however, the enzymes are still very different and catalyze different substrates (Wang *et al.*, 2018). CES1 is very common in the liver and is also expressed in adipocytes. CES2 is also expressed in the liver but is most abundant in the small intestine and colon (Wang *et al.*, 2018). Supposedly CES1 is responsible for 80% of the hydrolytic activity that takes place in the liver (Boonyuen, 2014).

1.2 Structure of carboxylesterase 1

The CES1 enzyme contains HIEL motifs at the C-terminus that is fundamental for the confinement of CES1 to the ER lumen. This confinement happens with help from the KDEL receptor localized in the ER membrane (Hosokawa, 2008). The binding of the CES1 enzyme to the ER membrane can be observed in figure 1A.

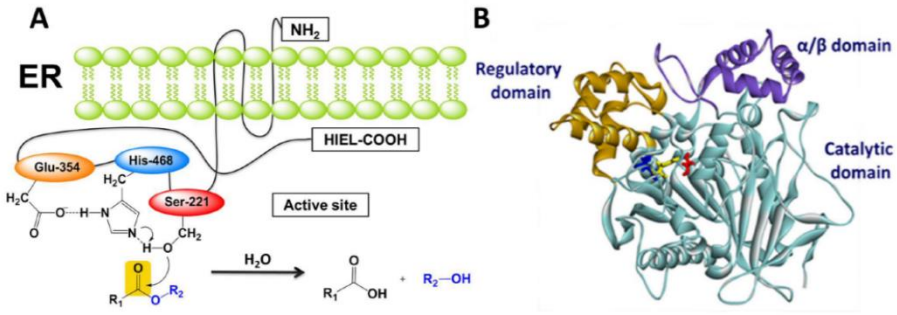

Figure 1: CES1 structural features including the HIEL-COOH motif bound to the KDEL receptor in the ER membrane (Hosokawa, 2008).

CES1 consists of 567 amino acids, and the molecular weight is 60 kDa (Rasmussen *et al.*, 2015) and is coated by hydrophobic amino acids, except for the catalytic triad (Wang *et al.*, 2018). The catalytic triad consists of Ser-221, Glu-354, and His-468 and can be observed in figure 1A. In its monomer form, the protein consists of three domains: the central catalytic domain, an α/β domain, and a regulatory domain (Wang *et al.*, 2018). The catalytic triad is placed in the interface of the three domains and is a crucial place considering the catalytic properties of CES1 (see figure 1B) (Wang *et al.*, 2018). The enzyme exists in an oligomeric structure of three 60 kDa units (see figure 2), which in turn are in equilibrium, which a hexameric form of the enzyme (Rasmussen *et al.*, 2015).

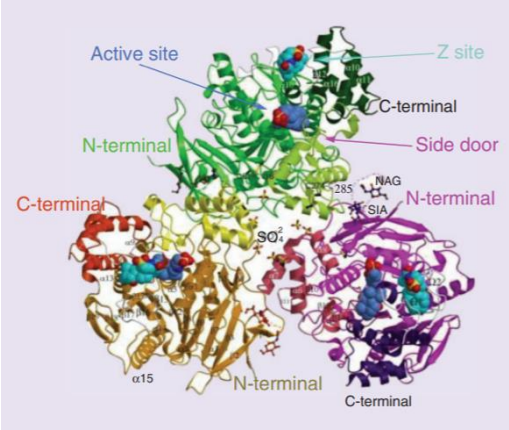

Figure 2: Structure of the CES1 enzyme in an oligomeric form (Rasmussen et al., 2015).

1.2.1 Central catalytic-, α/β-, and regulatory domains

The base in the central catalytic domain consists of α-helices and β-sheets. These secondary protein structures are as follows: helices α1–5, α9 and α13–15 and β1–9, β12–13, and β16–19 (Boonyuen, 2014). The reported crystal structure also shows that position Ans-79 CES1 consists of an N-linked glycosylation site (Boonyuen, 2014). This site is believed to assist in the folding of the protein, the stabilization of the trimer, and the solubility properties of the enzyme (Boonyuen, 2014). The central catalytic domain consists of an active site gorge, and it

is where the catalytic triad is located (Boonyuen, 2014). The active site, including the triad, is also a part of a ligand-binding site (Rasmussen *et al.*, 2015).

The α/β domain is surrounding the central catalytic domain (Boonyuen, 2014). The α/β domain function by supporting the subunit-subunit binding sites and the bulk of the hydrophobic internal structure (Holmes *et al.*, 2008).

The regulatory domain promotes the substrate binding and the release of product. Furthermore, this domain is also responsible for the trimer-hexamer equilibrium that CES1 exist in (Holmes *et al.*, 2008).

1.2.2 Ligand binding sites

According to the crystal structure, the enzyme contains three ligand binding sites. These sites are the active site, the side door, and the Z-site (Boonyuen, 2014). Located at the bottom of the central catalytic domain is the active site, and this area is also called the catalytic gorge or ligand-binding pocket (Boonyuen, 2014).

The catalytic gorge is split into two pockets - one rigid and one flexible - because of Ser-221 (Wang *et al.*, 2018). The structure of the pockets can be observed in figure 3. The rigid pocket makes CES1 selectable for substrates that contain a small acyl group (Wang *et al.*, 2018). The flexible pocket makes CES1 able to bind to esters with different acyl groups (Wang *et al.*, 2018). The larger flexible pocket also makes CES1 able to fit larger molecules such as cholesterol, and the pocket enables CES1 to hydrolyze many structurally different substrates (Hosokawa, 2008). The flexible pocket is bordering a secondary pore that can allow small molecules to enter and exit the active site (Hosokawa, 2008). This pore is known as the second ligand-binding site (the side door), leading to the active site (Boonyuen, 2014). It is considered possible that long acyl chains are oriented with extension through this secondary pore when they are catalyzed (Hosokawa, 2008). However, the side door's primary function is to transport small molecules into and out of the active site (Boonyuen, 2014).

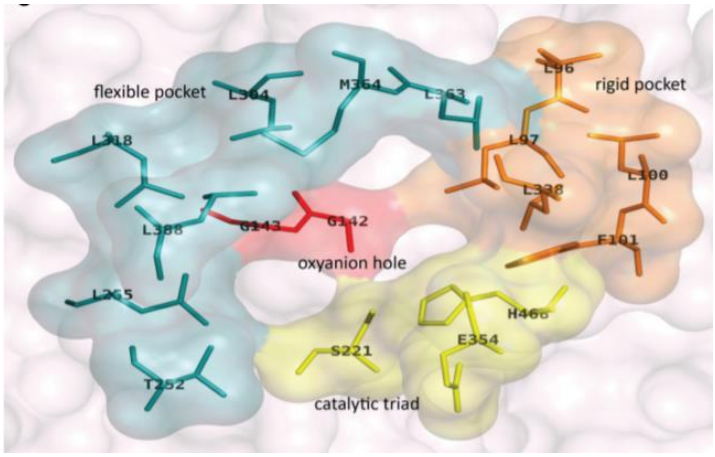

Figure 3: The flexible and rigid pocket in the CES1 enzyme. The two pockets surround the oxyanion hole, and the catalytic triad links the two parts (Nzabonimpa et al., 2016).

The third and last ligand binding site is the Z-site, and it is located on the surface of the enzyme (Boonyuen, 2014). This site is a central part of the trimer-heximer equilibrium that takes place for the enzyme, where the hexamer form consists of two trimers with their substrate-binding gorge facing toward each other (Boonyuen, 2014). This structure builds a dimer interface that, in turn, creates two loops called Ω1 and Ω2, and constructs a Z-shaped dimer with the Z-site hence the name (Boonyuen, 2014). It has been reported that many different compounds can bind to the Z-site as this binding side shows low affinity (Rasmussen *et al.*, 2015). The Z-site might also be involved in the allosteric activation of the enzyme (Boonyuen, 2014).

A supposed function of the Z-site has been reported. When a ligand binds to the Z-site, it promotes esterolytic activity by opening the enzyme so molecules can enter the enzyme through the catalytic pocket (Rasmussen *et al.*, 2015). This happens because it causes a shift in the trimer-hexamer equilibrium in favor of the trimeric state (Rasmussen *et al.*, 2015). However, the binding of a ligand might cause a change in the conformation in the catalytic pocket where hydrolysis is expedited (Rasmussen *et al.*, 2015), which supports the claim that the Z-site has an allosteric function.

1.3 Function of carboxylesterase 1

CES1's function concerns the catalytic triad Ser-221, Glu-354, and His-468 that cleaves the ester in a reaction containing two steps (Imai and Ohura, 2011). At neutral pH, the glutamate in the catalytic triad occurs in its charged form. This charge promotes the removal of a proton from histidine, which in turn results in serine transferring a proton to the opposite nitrogen of histidine (Imai and Ohura, 2011). This mechanism generates an oxygen nucleophile where the oxygen atom on the serine hydroxy group can attack the carbonyl carbon group of a substrate

(Imai and Ohura, 2011) (Hosokawa, 2008). This mechanism can be observed in figure 4. Hydrogen bonds between the negatively charged oxygen and the N-H group of two glycine molecules stabilize the oxygen (Hosokawa, 2008). This configuration is termed the oxyanion hole (Imai and Ohura, 2011), and can be observed in figure 3 and figure 4.

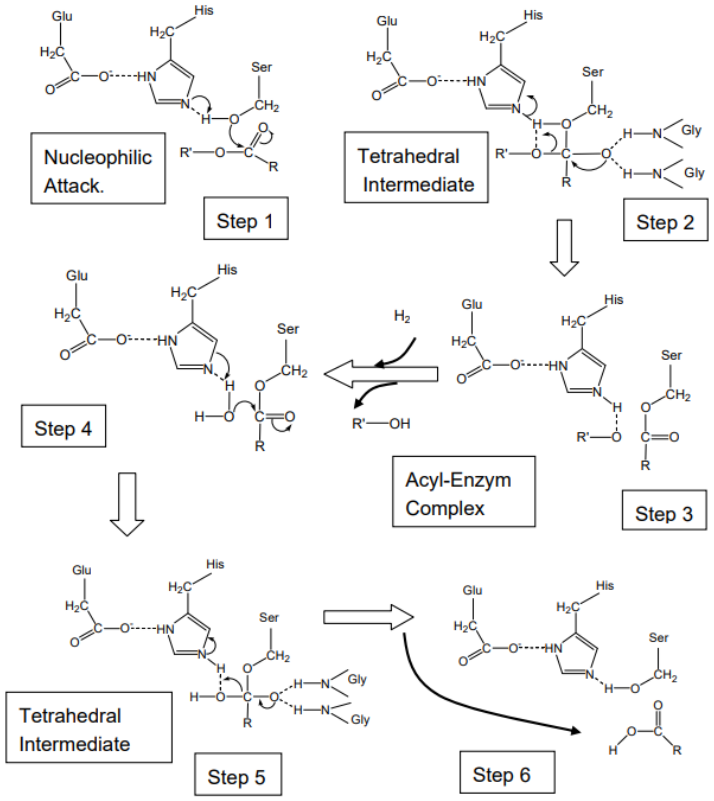

Figure 4: Oxyanion hole formed between the two Glycine and the oxygen molecule on the substrate (Hosokawa, 2008).

The next step contains an acid-catalyzed step where the ester bond is cleaved, and the leaving-group binds a proton from the imidazolium ion of His-450 (Hosokawa, 2008). Hence, the tetrahedral structure collapses and produces both an alcohol and an enzyme-acyl intermediate (Imai and Ohura, 2011). The alcohol unit then leaves the site, and the enzyme-acyl intermediate remains (Hosokawa, 2008). The histidine in the catalytic triad then actives a water molecule generating an attack on the acyl-enzyme intermediate, resulting in the formation of a new tetrahedral oxyanion intermediate (Imai and Ohura, 2011). Lastly, His-450 donates a proton to the oxygen atom connected to Ser-203, which results in the release of carboxylic acid that diffuses away, and the enzyme is ready to catalyze other substrates (figure 4, step 5-6) (Hosokawa, 2008), (Imai and Ohura, 2011).

1.4 Cathepsin A

Cathepsin A (CatA) is a lysosomal serine protease that acts as a carboxypeptidase (Schreuder *et al.*, 2014). The protein has several functions in the human body and is expressed in various human tissues, including kidney, liver, and lung (Hiraiwa, 1999). One molecule of cathepsin A is composed of 438 amino acid residues assembled into two subunits, cortical and apical (Minarowska *et al.*, 2012). The subunits are held together with disulfide bonds and form a monomer with a molecular mass of 52 kDa (Minarowska *et al.*, 2012). The protein has a protective function where it is linked with β-galactosidase and neuraminidase 1. This enzyme complex protects β-galactosidase and neuraminidase 1 against lysosomal degradation (Hiraiwa, 1999). Besides the protective function, CatA also has a catalytic role, including functioning as carboxypeptidase, deamidase, and esterase (Hiraiwa, 1999).

Lysosomal hydrolases are responsible for the degradation of macromolecules. More than 90% of all proteins are digested by lysosomal proteases, whereas cathepsins are the predominant proteases (Hiraiwa, 1999). The carboxypeptidase activity of CatA has an acidic pH optimum between 4.5 and 5.5 but shows deaminase and esterase activities at neutral pH (Schreuder *et al.*, 2014). CatA contains four disulfide bonds and one of them is suggested to play an essential role in creating a proper conformation for interaction with substrates implying that the enzyme has specific substrate specificities (Hiraiwa, 1999). The enzyme is a member of the α/β hydrolase fold family and shares similarities with other α/β hydrolases such as the cholinesterases and acetylcholinesterase (Hiraiwa, 1999). The enzyme hydrolyzes a variety of active peptides, but its exact function is still unknown (Schreuder *et al.*, 2014).

1.5 Prodrugs

Prodrugs are a structural modification technique that aims to improve the pharmacokinetic or pharmacodynamic properties of a drug (Abet *et al.*, 2017). These phases include solubility, permeability, absorption, distribution, and metabolic stability of the drug (Abet *et al.*, 2017). A prodrug is an inactive compound converted to an active drug by biotransformation, which can be enzymatic or non-enzymatic (Abet *et al.*, 2017). The metabolic transformation is necessary as it converts the prodrug into the active agent by catalyzation. The drug is catalyzed by specific enzyme, including the hydrolases CES1 and CES2 (Abet *et al.*, 2017).

1.5.1 The ProTide Technology and structure

The ProTide technology was pioneered by Chris McGuigan in the 1990s and has been developed as a prodrug approach to support efficient intracellular delivery of nucleoside analog (NA) monophosphates and monophosphonates (Mehellou, Rattan and Balzarini, 2018) (Jovanovic *et al.*, 2020). NA's are synthetic compounds that mimic their natural counterparts (nucleosides). The synthetic compound's incorporation alters the nucleic acid and inhibits cell division and viral replication, hence serving as an antimetabolite (Slusarczyk, Serpi and Pertusati, 2018). To exploit the therapeutic properties of NA's, they have to pass the cellular plasma membrane (Mehellou, Balzarini and McGuigan, 2009).

1.6 Nucleosides and nucleoside analogs

The building blocks of nucleic acids are nucleotides, which are the monomers in deoxyribonucleic acid (DNA) and ribonucleic acid (RNA) polymers (McMurry *et al.*, 2007, p. 813). Nucleotides are a composition of 2 moieties; a nucleoside and a monophosphate ester (Mahmoud *et al.*, 2018). A nucleoside is a nitrogenous base (purine or pyrimidine) linked to a 5'-carbon D-sugar-ring in deoxyribose and ribose in DNA and RNA, respectively, through a β-N-glycosidic bond. The purine bases, adenine and guanine, and the pyrimidine base, cytosine, are represented in DNA and RNA. However, pyrimidine thymine is only present in DNA, and uracil is exclusive in RNA (Mahmoud *et al.*, 2018). The general structure of a nucleoside, nucleotide, and the nitrogenous bases are listed in figure 5.

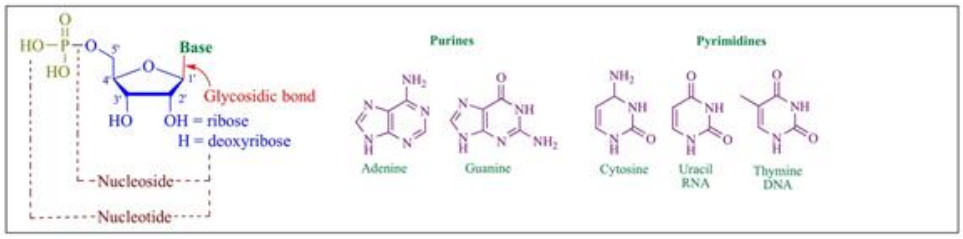

Figure 5: General structure of a nucleotide, a 5'-monophosphate ester of a nucleoside (Mahmoud et al., 2018).

Modifications in the sugar or nitrogenous base of nucleoside analogs (purines and pyrimidines) are possible and used to develop new drugs with biological activity (Mahmoud *et al.*, 2018). Modifications of the sugar moiety may include replacing the 4'-ring oxygen-atom with another atom, such as carbon, nitrogen, sulfur, or phosphorous. Replacement produces carbocyclic nucleosides, azanucleosides, thio-nucleosides, and phosphanucleosides, respectively. It is also possible to modify the sugar-ring with the addition of a heteroatom or changes in the sugar substituents, such as changes of the hydrogen or hydroxyl groups at positions 2', 3', and 4'. The outcome of these positions' changes has produced compounds with different biological activities (Mahmoud *et al.*, 2018). Furthermore, modification may also include changes in the sugar-ring size (Mahmoud *et al.*, 2018). Alterations, such as mentioned, may give rise to a variation in biological activity and selective toxicity due to the molecules' chemical and physical properties (Mahmoud *et al.*, 2018).

1.6.1 Synthesis of nucleotides and analogs

Deoxyribonucleotides and ribonucleotides are synthesized within the cells. There are no carrier proteins for them in the cell membrane, and the negatively charged phosphate groups prevent diffusion across the membrane (Van Rompay, Johansson and Karlsson, 2003). There are two pathways for deoxyribonucleotide, and ribonucleotide synthesis, called the *de novo*- and the salvage pathway (Van Rompay, Johansson and Karlsson, 2003). In the *de novo* ribonucleotide, ribonucleotides are synthesized from small molecules to ribonucleoside monophosphates and then further phosphorylated (Van Rompay, Johansson and Karlsson, 2003). *De novo* biosynthesis of purine nucleotides is complex, consisting of several enzymatic reactions. There are two salvage pathways for ribonucleotides. The first originates from free bases and then further phosphorylation through direct sugar-phosphate transfer (Van Rompay, Johansson and Karlsson, 2003). The second salvage ribonucleotide pathway is from ribonucleosides with further phosphorylation to their triphosphate form (Van Rompay, Johansson and Karlsson, 2003). Ribonucleosides and deoxyribonucleosides are imported into the cells by nucleoside transport proteins that facilitate diffusion or actively transport nucleosides across the

membrane. The phosphorylation from ribonucleosides to their ribonucleoside monophosphates is catalyzed by the ribonucleoside kinases (rNK), while the phosphorylation reaction of deoxyribonucleosides is catalyzed by deoxyribonucleoside kinases (dNK) (Van Rompay, Johansson and Karlsson, 2003). These kinases catalyze the first and often rate-limiting step of activating the nucleoside analogs. There are three known rNKs in human cells: adenosine kinase (ADK), uridine-cytidine kinase 1 (UCK1), and uridine-cytidine kinase 2 (UCK2) (Van Rompay, Johansson and Karlsson, 2003).

1.6.2 Masking of NA's

The ProTide technology involves methods in which the monophosphate–, and monophosphonate groups are masked, eluding the first phosphorylation steps (Alanazi, James and Mehellou, 2019) (Mehellou, Rattan and Balzarini, 2018). A general structure of ProTides illustrated in figure 6 shows an aryloxy phosphoramidate, and the nomenclature indicates the moieties, which are crucial functional groups, facilitating the NA's delivery process. The NA is masked by an aryl moiety and an amino acidyl moiety, N-linked as a phosphoramidate (Jovanovic *et al.*, 2020). The masking increases the lipophilicity, which increases the probability of the molecule diffusing across the plasma membrane. Once intracellular, the ProTide undergoes a series of metabolic steps, resulting in converting the inhibitor triphosphate (Jovanovic *et al.*, 2020).

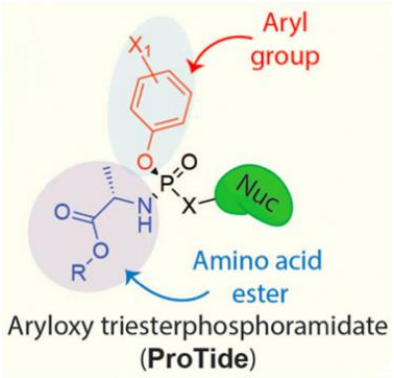

Figure 6: Above shows a general chemical structure of a ProTide. The highlights show the motifs; an aryl-group and an amino acid ester. The X, linked to the nucleoside analog (Nuc), can either be an oxygen atom (phosphoramidate) or a carbon atom (phosphonamidate). The X1 is an aromatic substitution. R on the amino acid ester can be any group *(Alanazi, James and Mehellou, 2019) (Wiemer and Wiemer, 2014)*.

1.7 Remdesivir

Remdesivir (GS-5734) is a ProTide of the nucleoside analog C-adenosine (figure 7) (Jovanovic *et al.*, 2020) (Reza Hashemian, Farhadi and Velayati, 2020). It was developed by Gilead Sciences, aiming to discover drug candidates against RNA viruses, specifically those who hold

potential as global pandemic inducers, including Ebola virus, Middle East respiratory syndrome (MERS), and severe acute respiratory syndrome (SARS) coronaviruses (CoV's) (Reza Hashemian, Farhadi and Velayati, 2020). Data screening results showed promising results using Remdesivir as an antiviral agent (Reza Hashemian, Farhadi and Velayati, 2020) (Siegel *et al.*, 2017). Furthermore, Agostini and colleagues reported in 2018 that Remdesivir could have inhibitory effects on human and zoonotic CoVs *in vitro* (Agostini *et al.*, 2018).

1.7.1 Structural features of Remdesivir and mechanisms of action

The active metabolite of Remdesivir, that reaches and acts upon the target, is the parent nucleoside, GS-441524 triphosphate (Yan and Muller, 2020). Intracellular delivery of the analog has been achieved by alteration of its bioavailability. An increase in lipophilicity, allowing the drug's entrance into the cell, attained by the ProTide technology, involves masking of the phosphate-group (Jovanovic *et al.*, 2020). Masking promotes the 5'-phosphate group to bypass the nucleoside kinase reaction, which is often associated with limited activity of nucleoside-based drugs (Jovanovic *et al.*, 2020). Remdesivir is dependent on host cellular metabolism in order to gain pharmacological activity (Mehellou, Rattan and Balzarini, 2018). By entrance into epithelial cells, including those of the lungs, Remdesivir is metabolized to a nucleotide triphosphate (figure 7), resulting in its active form (Reza Hashemian, Farhadi and Velayati, 2020). A schematic illustration of the steps is further described in figure 7. The first step involves cleavage of the amino ester in Remdesivir by esterases, resulting in a free carboxylate. Following this step may be cleavage by phosphoramidases to release the monophosphorylated nucleotide seen in figure 7.3. Subsequent enzymatic phosphorylation steps of the intermediate culminate in the pharmacologically active form of Remdesivir (figure 7.4) (Jovanovic *et al.*, 2020) (Yan and Muller, 2020).

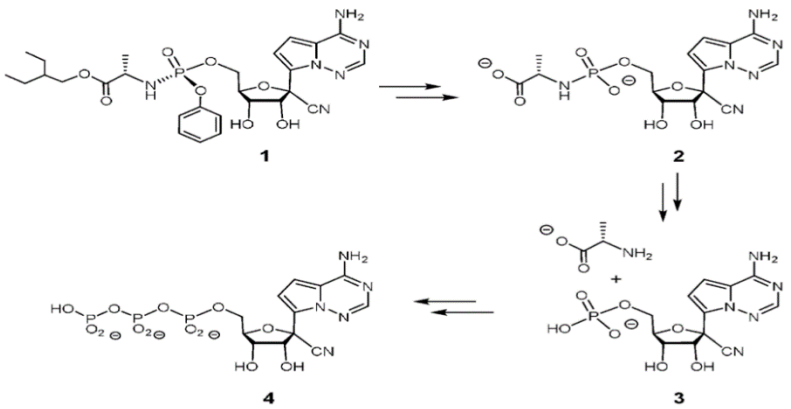

Figure 7: Upon human cell entrance, Remdesivir is enzymatically transformed to its triphosphate state (Reza Hashemian, Farhadi and Velayati, 2020). Proposed reaction scheme: 1: chemical structure of Remdesivir illustrating the C-nucleoside

analog and important moieties, pre-conversion. 2: Alanine metabolite derived from Remdesivir (1). 3: Hydrolysis aided by enzymes. 4: Enzymatic phosphorylation, resulting in a triphosphate. It is known that other ProTides have similar pathways during activation steps (Reza Hashemian, Farhadi and Velayati, 2020) (Jovanovic et al., 2020).

The active form of nucleoside analogs has the potential to prevent replication of multiple coronaviruses by inhibition of the viral RNA-dependent RNA polymerase (RdRp) (Reza Hashemian, Farhadi and Velayati, 2020). Inhibition of RdRp is achieved by the analog's competitive nature, as it competes with adenosine triphosphate, which is a naturally occurring molecule in cells. As the nucleotide analog is incorporated into the generating RNA strand, it causes a delayed stop in the viral elongation process (figure 8) (Reza Hashemian, Farhadi and Velayati, 2020). Moreover, the virus's exoribonuclease, which performs proofreading and correction of errors along the replicated RNA strands, cannot work against the nucleotide analog from Remdesivir (Reza Hashemian, Farhadi and Velayati, 2020).

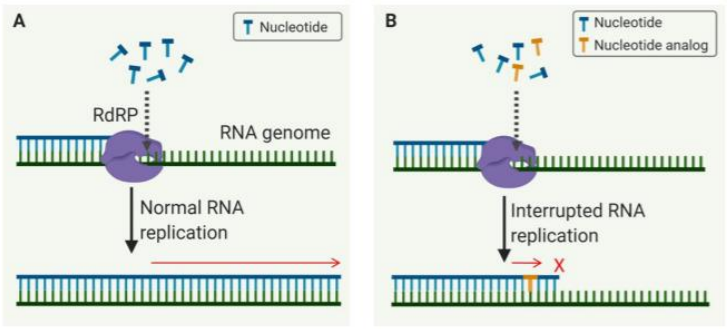

*Figure 8: **A)** RNA-dependent RNA polymerase (RdRp) replicates viral genome. **B)** Active nucleotide analogs causes premature termination of the generating viral RNA strand, hence working as an inhibitor (Zhu et al., 2020)*

Among the most crucial targets for antiviral agents are viral polymerases, and as cells do not express the viral RdRp's, they may be excellent targets. Positive-strand RNA viruses, such as those for SARS, the RdRp can be inhibited. The substrates for RdRp's are ribonucleoside triphosphates (NTP's), and nucleoside analogs compete with NTP's (Jovanovic *et al.*, 2020). When antiviral drugs are administered, such as Remdesivir, the active form incorporates during viral RNA generation and eventually causes early or delayed chain termination, as illustrated in figure 8 (Reza Hashemian, Farhadi and Velayati, 2020).

2.0 Laboratory introduction

The project concerns laboratory work in which the aim is to produce *in vitro* recombinant CES1 and CES2 enzymes. Only CES1 enzymes are refolded and checked for enzymatic activity by using a broad-spectrum esterase substrate (4-nitrophenyl acetate).

The following section aims to give a brief theoretical orientation about bacterial protein expression. A subsection is dedicated to reviewing applied laboratory methods, and a presentation of the obtained result will be introduced and discussed in relation to the article by Boonyuan et al. (2015).

2.1 Transformation: Expression of CES1 and CES2

Scientists are able to exploit bacteria's ability to take up fragments and incorporate it in their genome (Griffiths *et al.*, 2012, p. 163). This process is known as transformation and is a useful mechanism that allows bacteria to gain new functions such as resistance to antibiotics (Doghaither and Gull, 2010). Based on this, it is possible to insert a gene of interest into a plasmid (Griffiths *et al.*, 2012, pp. 368–369). These specially designed plasmids are called vectors, and they are often engineered to only carry the most essential fraction needed for cloning (Lodish, Berk and Zipursky, sec. 7.1). Hence, vectors only carries the gene of interest, a replication origin, and a drug-resistance gene (Lodish, Berk and Zipursky, sec. 7.1). These specially engineered vectors are then added to a bacterial culture, where the bacteria can absorb the plasmid as it carries genes that are favorable for survival (Griffiths *et al.*, 2012, p. 368). After uptake, the bacteria now contain the plasmid and thereby the gene of interest which then will be cloned and amplified as the bacteria multiply (Griffiths *et al.*, 2012, p. 368). Because vectors are designed to carry a resistance gene, scientist can confirm that only bacteria who absorbs the plasmid survives by adding the exact antibiotic (Doghaither and Gull, 2010)

2.2 Bacterial transformation

The gene for T7 RNA polymerase is inserted into the chromosome of E. Coli and transcribed from the lac promoter (Cox, Doudna and O'Donnell, 2015, p. 697). The *lac* operon is the gene sequence that encodes the proteins for the breakdown of lactose. In E. coli, the repressor is bound to the operator making the promoter inactive. This occurs because E. coli prefers glucose from lactose when glucose is present (Cox, Doudna and O'Donnell, 2015, p. 697). Since lactose is naturally involved in E. coli metabolism, E. coli possesses the entire *lac* operon and is also capable of producing the repressor (Cox, Doudna and O'Donnell, 2015, p. 698). By not having lactose in the medium, E. coli will not express the genes regulated by the lac operator (Cox,

Doudna and O'Donnell, 2015, p. 697). The repressor can be released from the operator with the substance isopropyl β-D-1-thiogalactopyranoside (IPTG) (Cox, Doudna and O'Donnell, 2015, p. 699). If IPTG is added to the growth medium, E. coli will begin to express the genes that encode the breakdown of glucose, but also the genes on the vector. The genes are only expressed if the inducer IPTG is added (Cox, Doudna and O'Donnell, 2015, p. 699). The lac operator between the T7 promoter and the cloned gene will reduce transcription of the cloned gene in the absence of IPTG (Cox, Doudna and O'Donnell, 2015, p. 699).

2.3 Michaelis-Menten

Enzymatic activity can kinetically be described by the Michaelis-Menten rate equation:

$$v_0 = \frac{V_{max} \cdot [S]}{K_m + [S]}$$

where v_0 is the initial rate of the reaction. V_{max} is the maximum velocity of the reaction, and [S] is the concentration of the substrate. In the following experiment, the substrate used is 4-nitrophenyl acetate. Finally, K_m is the Michaelis-constant which describes the concentration of the substrate when v_0 is equal to the half of V_{max}. In total the equation describes the relationship between initial velocity and the substrate concentration (Moran *et al.*, 2014, pp. 176–177).

3.0 Methods

The following section reviews the applied methods during the laboratory work of this project. The section is divided into three experiments and they are as follows: protein expression, protein purification and protein refolding and enzyme activity measurement. The sections will describe the aim of each experiment and present the materials and methods used, making it possible to replicate.

3.1 Experiment 1: Protein expression

The aim of the protein expression experiment was to transfer plasmids containing genes coding for human CES1 and CES2. To complete this we worked with competent BL21(DE3) C41 *Escherichia coli* (E. coli). Before proceeding with adding plasmids to the E. coli, LB medium was prepared and the procedure can be found in Appendix. Furthermore, an array of buffers where used, and preparation of these are also listed in Appendix. To compile the above, materials and procedures listed below, was used.

3.1.1 Materials for protein expression

0,5 µL plasmid for CES1, 0,5 µL plasmid for CES2, 2x 10 µL competent E. coli cells, 2x 1 mL LB medium, 8x 50 mL LB medium, 8x 50 µL kanamycin

3.1.2 Method for protein expression

In one sterilized 1,5 mL Eppendorf tube we added 0,5 µL plasmid for CES1 and 10 µL competent E. coli cells. The same procedure was done for CES2. The mixture was heat shocked at 42 °C for 1 minute exactly. Next, 1 mL LB medium was added to each Eppendorf tube, and left for incubation in a shaking water bath at 400 rounds per minute (rpm) at 37°C for 60 minutes. We followed that by transferring the inoculates to 100 mL autoclaved flasks and added 50 mL LB medium and 50 µL kanamycin. The mixture was left overnight in a shaking water bath at 37°C.

The next day, we transferred 10 mL of the overnight inoculates to 800 mL autoclaved flasks. We repeated this 4 times per plasmid. To each flask, 400 mL fresh LB medium was added. As the added kanamycin was insufficient, we decided to add an additional 400 µL to each flask and left it on the shaking water bath at 37°C for 1,5 hour or until we obtained an OD_{600} at 0,6 - 1. We sampled both CES1 and CES2 for OD-measurement and when each had reached OD_{600}

= 0,8, we induced the cells by adding 200 µL 1M ITPG to the flasks. Next, the flask was left to incubate overnight at 25°C in a shaking water bath at 110 rpm.

The following day the aim was to separate the cell culture from the medium. We harvested the cells by centrifugation at 1000xg for 10 minutes and then 2000xg at 10 minutes. The results were not sufficient, so we centrifuged again at 2000xg for 10 minutes. Afterwards, the cells were frozen in the centrifuge tubes at – 20 °C.

3.2 Protein purification of CES1 and CES2

The aim of the second step of the laboratory work was to purify our protein of interest. To accomplish this an array of different buffers was prepared and the producer for these are listed in Appendix. Both a nanodrop and an SDS-PAGE was used to confirm the purification of CES1 and CES1.

3.2.1 Materials for protein purification

Lysis buffer, buffer A, elution buffer, wash buffer, Ni-NTA, SDS-PAGE, SDS buffer, loading buffer, Tissue Lyser and a buffer to reduce protein interaction (RPI-buffer).

3.2.2 Methods for protein purification

An array of buffers was prepared before the purification step, including lysis buffers (buffer A and RPI buffer), wash and elution buffers. The preparation of buffers and the concentration are sectioned in Appendix.

The cell pellets were taken from the freezer and resuspended in lysis buffer and disrupted by a Tissue Lyser. The cell lysate was centrifuged at 20.000xg at 4°C for 10 minutes, and the supernatant was removed. The pellet was washed with RPI-buffer and centrifuged at 20.000xg at 4 °C for 10 minutes. The supernatant was collected, and the pellet was left in the freezer to be used for SDS-PAGE later on. The supernatant was collected in 2x 15 mL tubes and incubated with 1 mL Ni-NTA to allow our protein of interest to bind to the Ni-NTA. Buffer A was also added to the tubes. The unbound proteins were removed by adding wash buffer and incubating for 2 minutes under shaking. The tubes were centrifuged at 1000xg and then at 2000xg, and the supernatant was removed. This was repeated two times. Afterward, the elution buffer was added to the tubes. The tubes were incubating for 2 minutes under shaking and centrifuged again at the same speed as the washing step. The supernatant was collected in new tubes, and the step was repeated three times. This resulted in a total of 12 tubes, 6 with CES1

containing 2x Elution 1, 2x Elution 2, and 2x Elution 3, and the same for CES2. Expecting the first and second elutes of the samples to contain highest concentrations of our protein of interest, these were measured on the nanodrop. These results can be observed table 1 below.

Table 1 – Nanodrop measurements of elution samples		
	E1	E2
CES 1	-0,032 mg/mL	-0,011 mg/mL
CES 2	-0,052 mg/mL	-0,017 mg/mL

Before refolding, recombinant CES1 and CES2, SDS-PAGE was performed to investigate if we had succeeded in protein purification. The results from the nanodrop suggest that the purification had failed, as the results were negative. However, the SDS-PAGE would illustrate if our samples contained protein, and if not, where they might have been lost during the procedure.

The first well was loaded with a protein molecular weight marker. Well two and three were cells before IPTG was added, well 4-5 contained the pellet after using the Tissue Lyser and centrifugation at 20.000xg at 4°C for 10 minutes after RPI-buffer was added. Well 6-7 contain the supernatant from the cell lysate after the first centrifugation. Next, the supernatant from the washing step was added, and the last 6 wells contained the elution of CES1 and CES2. A picture of the gel can be seen below.

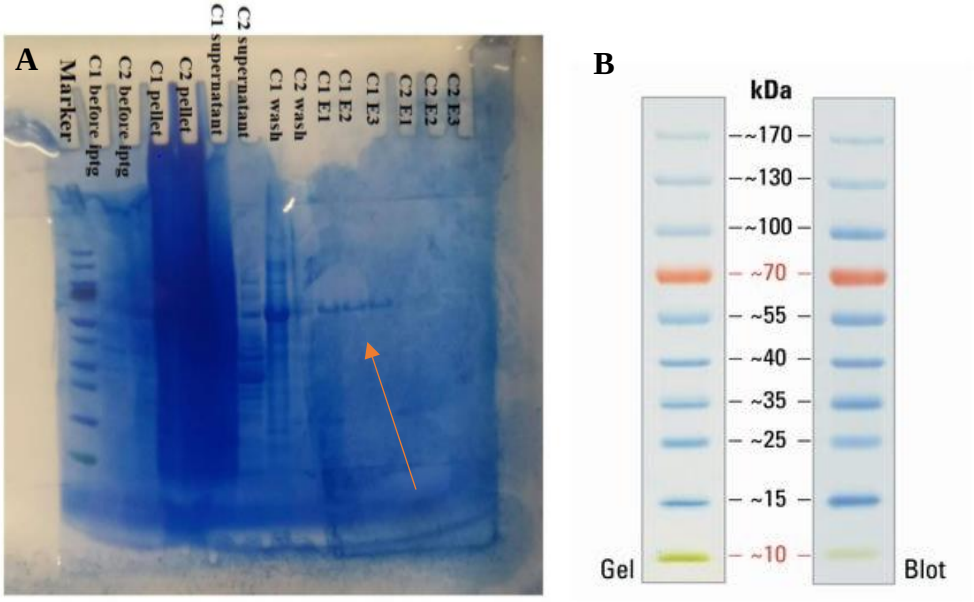

Figure 9: A) Picture of obtain SDS-PAGE results from the laboratory. The arrow indicates the elution samples. B) Protein latter for the used marker in SDS-PAGE.

3.2.3 Data processing for protein purification

Based on the marker and the fact that CES1 and CES2 both are around 60 kDa, the gel indicates the presence of CES1 in all three elution samples (Figure 9A). However, CES2 cannot be observed in the last three rows. Looking at the rows containing the washing buffer, a band can be observed for CES1, indicating fractions of the protein was lost during this step. The same can be noticed for CES2, but the band is smaller and difficult to see. This implies that CES2 was lost earlier in the procedure. Therefore, the rest of the experiment continued with the use of CES1 alone.

3.3 Enzyme refolding and activity

The last step of the experiment aimed to refold and test the activity of CES1. Based on the results from the SDS-PAGE, CES1 was indicated to be present in the elution samples. Four different refolding solutions were made, and buffer exchange was performed. Finally, the enzyme activity was measured by using 4-nitrophenyl acetate as the substrate. The reaction for the substrate is illustrated in figure 10.

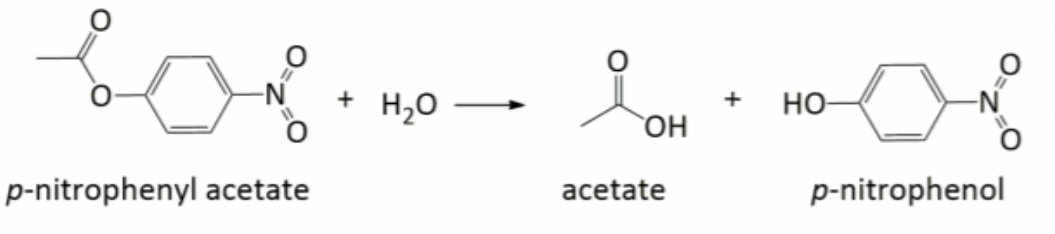

Figure 10: 4-nitrophenyl acetate hydrolysis by CES1 (Huang *et al*., 2016)

3.3.1 Materials for refolding of recombinant CES1

Tris-HCl buffer (pH = 7,5), β-mercaptoethanol, glycerol, glucose, Eppendorf tubes, Ultra Centrifugal Filter Units, 4-Nitrophenol-acetat, acetonitrile, 96-well plate.

3.3.2 Methods for refolding of recombinant CES1

For the refolding of CES1, four refolding solutions were prepared. These contained Tris-HCl buffer, β-mercaptoethanol, and either 1% or 10% glucose or glycerol. The procedure for the refolding solutions is listed in Appendix.

A trial solution was made to test the refolding where the CES1 Elution 1 sample was used. We transferred 4x 100 μL and 4x 200 μL of CES1 E1 to 8 1,5 mL Eppendorf tubes. 900 μL of the

trial solution was added; thus, each of the four solutions was added to Eppendorf tubes containing 100 and 200 μL of CES1 E1. The tubes were placed on ice for 30 minutes and spun down. Then absorbance was measured on the nanodrop. The results are showed in Table 2 below:

Table 2 – trial 1 of refolding of CES1 Elution 1		
	100 μL CES1	200 μL CES1
1% Glycerol	0,033 mg/mL	0,064 mg/mL
10% Glycerol	0,040 mg/mL	0,065 mg/mL
1% Glucose	0,029 mg/mL	0,043 mg/mL
10% Glucose	0,040 mg/mL	0,078 mg/mL

Another sample was made, this time containing 1 mL of CES1 E1 and 9 mL of the different trial solutions. The results from the nanodrop were similar to the trial solution and can be viewed in Table 3.

Table 3 – refolding of CES1 Elution 1	
	1 mL CES1
1% Glycerol	0,032 mg/mL
10% Glycerol	0,032 mg/mL
1% Glucose	0,034 mg/mL
10% Glucose	0,040 mg/mL

The four refolding solutions with a volume of 10 mL was left in the fridge for 17 days. The experiment then continued with buffer exchange. First, the refolded samples were transferred to four Ultra Centrifugal Filter Units. The tubes were centrifuged at 2000xg for 5 minutes. This was evaluated as ineffective. Therefore, the tubes were centrifuged again at 3000xg for 10 minutes. Then the remaining solution was added to the tubes, and they were centrifuged at 3000xg for 15 minutes.

3 mL Tris-HCl buffer was added to the four tubes to start the buffer exchange and remove urea and imidazole. The tubes were centrifuged again at 3000xg for 10 minutes, and the flow-through was removed. This step was repeated. The absorbance was then measured on the nanodrop, and the results are listed in Table 4 below.

Table 4 – Nanodrop results before enzyme activity measurement	
Glucose 1%	0,010 mg/mL
Glucose 10%	0,001 mg/mL
Glycerol 1%	-0,04 mg/mL
Glycerol 10%	0,047 mg/mL

Only the two highest concentrations were used for the enzyme kinetics assay. This was the sample with 1% glucose and 10% glycerol. This was done due to the time limit. The substrate 4-nitrophenyl acetate was dissolved in acetonitrile to obtain a concentration of 100mM. A 96-well plate was used for the activity assay. 180 µL Tris-HCl and 8 µL 96% ethanol was added to 12 wells. 1, 2, 4 and 8 µL of the dissolved substrate was added to three wells each. 20 µL CES1 with 1% glucose was added to the first four wells, containing 1, 2, 4 and 8µL of the dissolved substrate, and 20 µL CES1 with 10% glycerol was added to the next four wells. Lastly, 20 µL Tris-HCl was added to four wells as a control. The plate was read by a spectrophotometer and absorbance was measured for 15 minutes. An illustration of this procedure can be observed on figure 11.

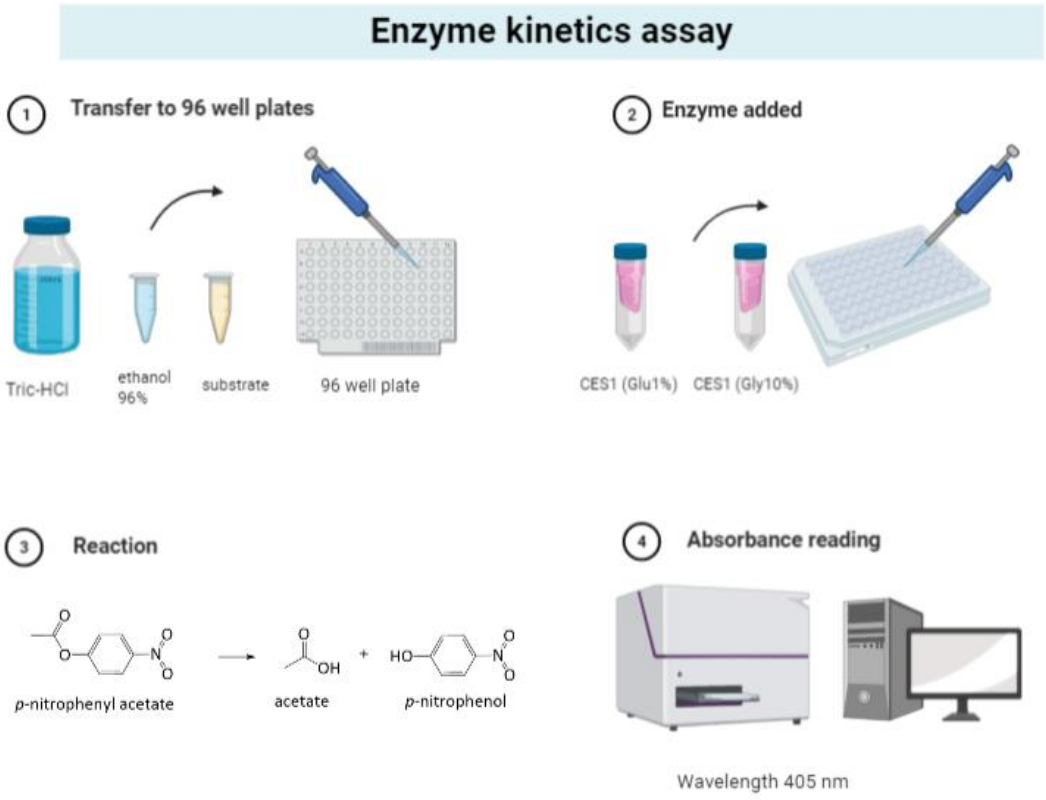

Figure 11: Illustration of enzyme kinetic procedure. Picture modified in BioRender.

3.3.3 data processing for enzyme kinetics.

The measured absorbance and time were plotted in excel and can be observed below.

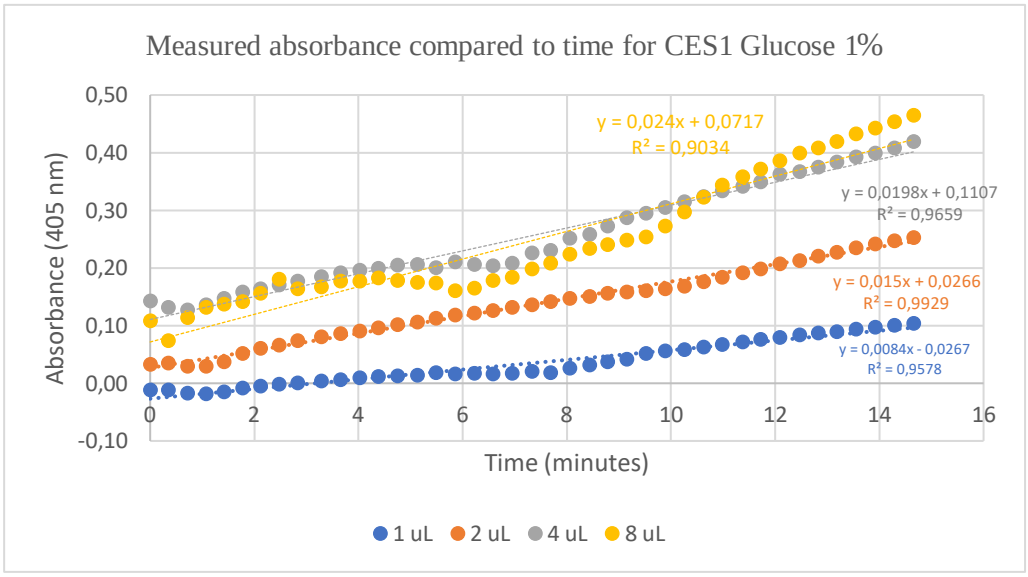

Figure 12: The four substrate concentrations plotted against time for Glucose 1%. The values are in µL (uL).

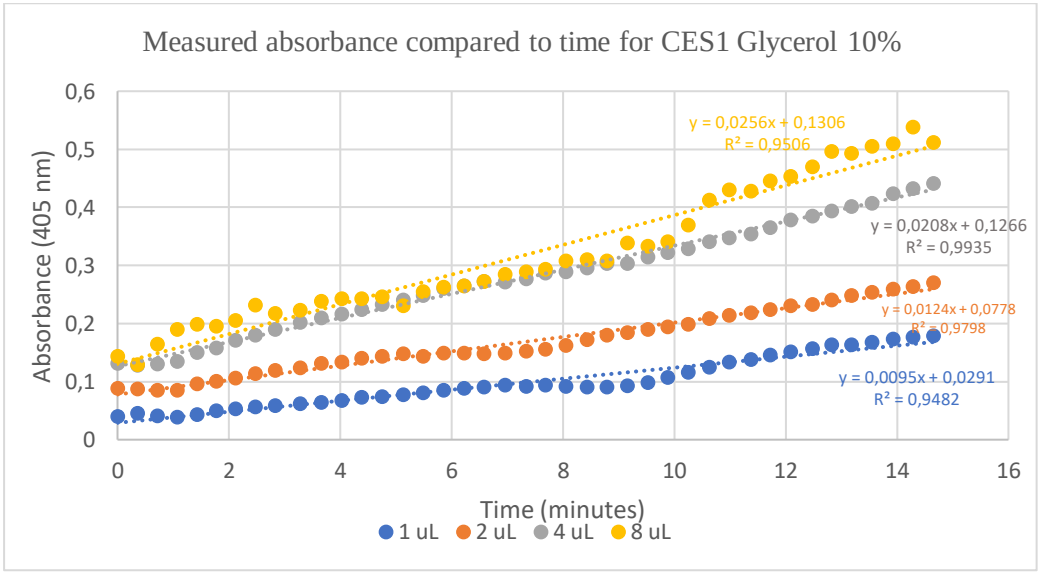

Figure 13: The four substrate concentrations plotted against time for Glycerol 10%. The values are in µL (uL).

The obtained values were used to calculate the slope. The slope for each of the concentrations was dived with the molar extinction coefficient which was found to be 18 mM according to the article "*Efficient in vitro refolding and functional characterization of recombinant human liver carboxylesterase (CES1) expressed in E. Coli*" (Boonyuen *et al.*, 2015). This was done to calculate the velocity in mM/min. The values were multiplied by factor 1000 to transform the unit to µM. The data can be observed in Table 5 and 6.

Table 5: Listed values for velocity and substrate concentration for CES1 Glucose 1%					
Substrate	Slope	$v = slope/\varepsilon$	$v \cdot 1000$	Substrate concentration (mM)	Substrate concentration (µM)
1 µL	0,0084	0,00047 mM/min	0,467 µM/min	0,354	354
2 µL	0,015	0,00083 mM/min	0,833 µM/min	0,69	690
4 µL	0,0198	0,00110 mM/min	1,10 µM/min	1,38	1380
8 µL	0,024	0,00133 mM/min	1,33 µM/min	2,76	2760

Table 6: Listed values for velocity and substrate concentration for CES1 Glycerol 10%					
Substrate	Slope	$v = slope/\varepsilon$	$v \cdot 1000$	Substrate concentration (mM)	Substrate concentration (µM)
1 µL	0,0095	0,00053 mM/min	0,528 µM/min	0,354	354
2 µL	0,0124	0,00069 mM/min	0,689 µM/min	0,69	690
4 µL	0,0208	0,00116 mM/min	1,156 µM/min	1,38	1380
8 µL	0,0256	0,00142 mM/min	1,422 µM/min	2,76	2760

The enzyme velocity and substrate concentration were plotted and can be seen in section 4.0

4.0 Results

Based on the laboratory work, CES1 was expressed via a plasmid transfer to E. coli. The enzyme was later purified. The results from the nanodrop showed low amount of protein in the samples. However as some of the results were negative, it is unsure how precise these measurements were. The SDS-PAGE indicated that CES1 was present in the elution samples. Based on this, the elution samples were refolded.

To test if the experiment succeeded the enzyme activity was investigated by adding 4-nitrophenyl acetate as this is a known substrate for CES1. The enzyme velocity was calculated based on the absorbance measured at four different concentrations.

Based on a Michaelis-Menten plot V_{max} and K_m may be estimated by reading the graph (marked with orange).

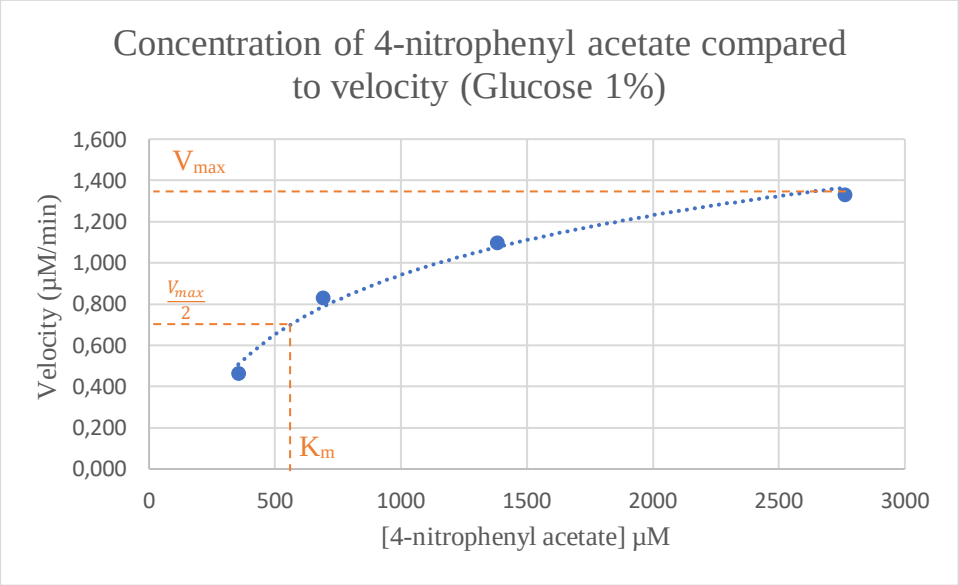

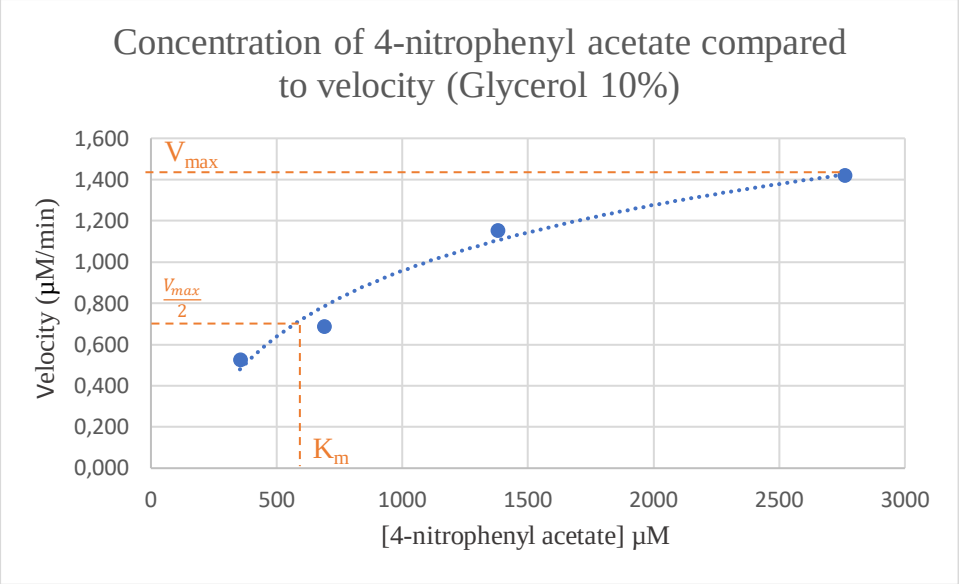

For CES1 with 1% glucose, V_{max} is estimated to be 1,39 µM/min and K_m is estimated to be 570 µM. For CES1 with 10% glycerol V_{max} is estimated to be 1,4 µM/min and K_m is estimated to be 580 µM.

4.1 Discussion of laboratory work

In the article by Boonyuen et al. (2015) the team includes a Michaelis Menten plot from their CES1 sample containing 1% glycerol (see figure 14). They reported a K_m value at 579 ± 79µM and a V_{max} at 73 ± 4 µM/min/mg. Looking at our, results obtained from the enzyme activity experiment, our two K_m values (570 and 580 µM) are very similar to the one reported by Boonyuen et al. (2015). This supports the validity of our obtained K_m and uphold the claim that we succeeded in purifying functional CES1. However, it is important to mentioned that Boonyuen et al. (2015) also reports a standard deviation of 79 µM, indicating some variation in their results. Our experiment was only run once due to time limit and we therefor have no standard deviation to report. This might give a distorted view of our data, as running an experiment once is biased and is prone to error.

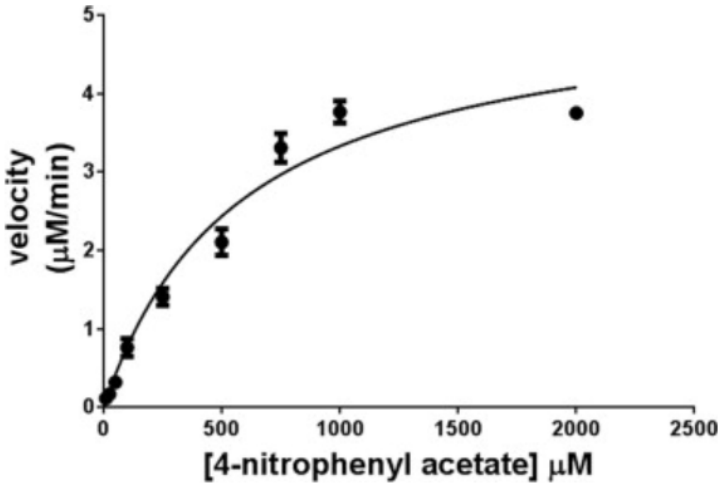

Figure 14: Michaelis Menten plot based on results from Boonyuen and collogues (Boonyuen *et al*., 2015).

Looking at figure 14, Boonyuen et al. (2015) reached a velocity around 4μM, and compared to our obtained data, and it was 285% higher. The low velocity might be caused by prolonged storage in the fridge, a total of 17 days after the refolding procedure. The effect of this is unknown, but it might have affected the enzyme activity. However, the laboratory work aimed to express and purify recombinant CES1 and CES2. Based on the activity of CES1, we concluded that the protein had been purified successfully. As mentioned earlier, CES2 purification was not succeeded.

5.0 Literary search

The analysis consists of an array of articles, all collected by search strings on PubMed on different dates. All search strings were sorted by language to only show articles written in English. The first string was searched on 24th of November, and was as follows:

((((CES1) AND (human)) AND (antiviral)) AND (carboxylesterase 1)) AND (metabolism).

The words "carboxylesterase 1" and "CES1" was chosen to widen the search by using the formal name and the most common abbreviation. The choice of keywords was based on interest of whether CES1 hydrolyze antivirals and to collect information regarding the metabolism of antivirals by CES1. "Human" and "Metabolism" was chosen because the focus of this project is to investigate metabolism of ProTides in humans.

The search string resulted in 25 hits of which 2 were relevant for the scope of this project. The remaining articles were either irrelevant or did not contain any useful information for this project. Based on the poor relevance of articles another search string was made on the 30th of October and were as follows:

(nucleoside gs-441524) AND (remdesivir)) OR (tenofovir metabolism carboxylesterase)

The aim was to find articles that concerns the metabolism of Remdesivir and therefore, the keywords "gs-441524" and "Remdesivir" was chosen. Furthermore, as there are few articles concerning this topic the search string also contained the keywords "tenofovir metabolism carboxylesterase" to find articles about this prodrug.

The aim of the analysis is to bring forth relevant experimentally gained data, and to highlight proposed metabolic pathways of two well studied antiviral ProTides, Sofosbuvir and Tenofovir. This project aims to use obtained information to discuss the possible metabolic activation pathways for Remdesivir, which is currently unknown.

Based on the search strings above, 3 articles were found relevant and are listed below:

- *"Intracellular Activation of Tenofovir Alafenamide and the Effect of Viral and Host Protease Inhibitors"* by Birkus et al. (2016).
- *"Implications of Efficient Hepatic Delivery by Tenofovir Alafenamide (GS-7340) for Hepatitis B Virus Therapy"* by Murakami et al. (2015).
- *"Mechanism of Activation of PSI-7851 and Its Diastereoisomer PSI-7977"* by Murakami et al. (2010).

6.0 Analysis of literature

A total of 3 articles is included in the analysis. The focus is to investigate the reported enzymes involved in the activation of ProTides, including Sofosbuvir and Tenofovir, and reflect those on the still unknown activation of Remdesivir. In this section we review the different methods described in the articles and examine their obtained data. These will later be used for comparison and ultimately be included in a proposed metabolic activation pathway of Remdesivir. Both Sofosbuvir and Tenofovir serve the same purpose as Remdesivir: intracellular delivery of nucleoside analogs as means for antiviral effects (Murakami *et al.*, 2010) (Murakami *et al.*, 2015) (Birkus *et al.*, 2016).

6.1 Introduction to results from the literature analysis

As mentioned in sections above, the analysis consists of three articles. Two articles focus on Tenofovir Alafenamide, a prodrug of the anti-hepatitis drug, Tenofovir. The final article is about the activation of Sofosbuvir (PSI-7851).

In the article *"Intracellular Activation of Tenofovir Alafenamide and the Effect of Viral and Host Protease Inhibitors"* by Birkus et al. (2016) and *"Implications of Efficient Hepatic Delivery by Tenofovir Alafenamide (GS-7340) for Hepatitis B Virus Therapy"* by Murakami et al. (2015) a set of enzymes were reported to be involved in the metabolism and activation of Tenofovir Alafenamide (TAF). The results obtained by Murakami et al. (2015) showed a high level of the pharmacologically active metabolite of TAF in human primary hepatocytes. The team reported CES1 as being the primary hydrolyzing enzyme, while CatA had a minor contribution. These results were interpreted by high intracellular levels of the metabolite TAF-DP. For further confirmation of the role of CES1 and CatA in the hydrolyzation, the team inhibited both enzymes and observed a decline of the metabolite. Moreover, the team attributes a high cellular permeability of the ProTide to the masking of the negative charges on the phosphonate, which increases the lipophilicity, and may result in higher TAF levels. As opposed to Murakami et al. (2015) conclusion in which CES1's primary contribution to the hydrolysis in TAF's metabolism, Birkus et al. (2016) credits CatA as the major contributor. During an experiment with overexpression of CatA or CES1, the team observed intracellular hydrolysis of TAF at 2- and 5-fold, respectively.

A further analysis of CatA knockdown expression in HeLa cells, Birkus et al. (2016) reported that TAF metabolism was reduced by 4-fold. In conclusion, the team provide results of which

CatA is the major hydrolase in the intracellular activation of TAF (Birkus *et al.*, 2016). In the study by Murakami et al (2015), a similar result is reported. The study concerns the activation of TAF in primary human hepatocytes and Murakami et al. (2015), reports that CES1 is highly expressed in the liver (Murakami *et al.*, 2015). Based on the obtained results by inhibition of both CES1 and CatA, Murakami et al. (2015) concludes the involvement of both enzymes in activation of TAF in the liver cells (Murakami *et al.*, 2015). However, it can be discussed whether experiments with cells lines can be transferred to the to human body, as the complexity far extends the simplicity of a cell model.

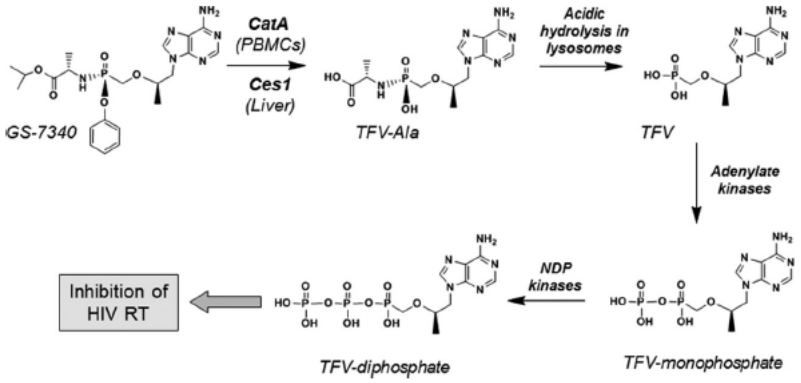

Figure 15: Intracellular metabolic pathway of TAF (Birkus et al., 2016)

Above is the metabolic activation pathway of TAF (Birkus *et al.*, 2016). As the first step implies, CatA and CES1 are responsible for the activation of TAF. However, it is important to note that the team discriminates their stand according to tissue or location of the hydrolyzation event. CatA is indicated as a hydrolase in the peripheral blood mononuclear cells (PBMC's), whereas CES1 is supposed to be the hydrolyzation contributor in the liver.

In the final article, *"Mechanism of Activation of PSI-7851 and Its Diastereoisomer PSI-7977"*, the team investigates the activation of the ProTide, Sofosbuvir (PSI-7851) by examining the enzymes involved (Murakami *et al.*, 2010). The aim was to report the mechanism of activation of Sofosbuvir. The results indicate that the hydrolases CatA and CES1 is responsible for the hydrolyzation in Sofosbuvir. Murakami et al. (2010) reported neutrophil elastase, CatA, and CES1 as possessing hydrolyzing properties regarding Sofosbuvir. The data support similar results obtained by Birkus et al. (2016) and Murakami et al. (2015) but only for the involvement of CatA and CES1 in the activation of TAF and Sofosbuvir. Neutrophil elastase was excluded for further analysis as the enzyme is not present in hepatocytes (Murakami *et al.*, 2010). Below is the chemical structure of Sofosbuvir (figure 16A).

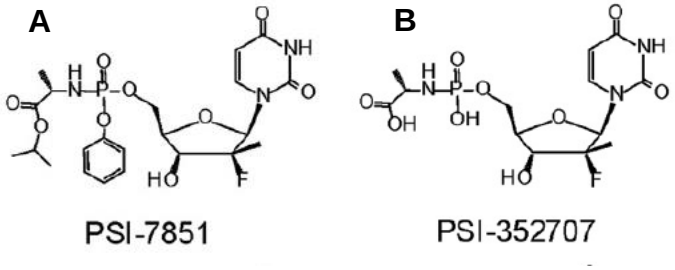

Figure 16: A) The chemical structure of Sofosbuvir (PSI-7851). B) Intermediate of Sofosbuvir (Murakami et al., 2010).

Murakami et al., 2010 use an array of experiments to investigate the initial activation step, the intermediate products and the final, active triphosphate of Sofosbuvir.

The subsequent product after the initial hydrolyzation by CatA and/or CES1 is PSI-352707 (figure 16B). Similar to TAF, it is the same group of the phosphonate that is hydrolyzed. The results are based on experiments involving human primary hepatocytes. The team also emphasize that the hydrolysis of the ester is followed by a putative nucleophilic attack on the phosphorous by the carboxyl group, a mechanism explained in section 1.3 and in figure 4. Consequently, this leads to spontaneous removal of the phenol group.

6.2 Experimental methods from the articles

All three articles report using hepatocytes in at least one experiment, which is plausible since the drugs are anti-hepatitis. The article shares some similarities but has distinct differences. As mentioned, Murakami et al. (2015) and Birkus et al. (2016) both study the metabolism of TAF, where Murakami et al. (2015) report the involvement of CES1 in the liver. The team also performed an *in vivo* experiment. The experiment included dogs, which had TAF orally administered for 7 days (Murakami *et al.*, 2015). The team observed high levels of the TAF metabolite TFV-DP in the liver and observed a decline of TAF in plasma proportionally with the development of the active TFV (Murakami *et al.*, 2015).

In contrast to Murakami et al. (2015), Birkus et al. (2016) used HEK292T cells. Birkus et al. (2016) overexpressed 11 different enzymes and studied the levels of intracellular metabolites. The team also conducted an experiment with knockdown CatA in HeLa cells. Results showed a 5-fold decrease in intracellular TAF metabolism. Lastly, an experiment to further analyze the involvement of CatA in the metabolism of TAF, the team used known inhibitors for the enzymes in primary human CD4+ cells. The team observed that the concentration of CatA inhibitors was proportional with the decrease in anti-HIV activity. Based on the 11 enzymes

the team studied, only CatA and CES1 showed a significant change in intracellular metabolites. The team also reported that CES2 was not able to hydrolyze TAF *in vitro* (Birkus *et al.*, 2016)

Murakami et al. (2010) use similar methods as Murakami et al. (2015) and Birkus et al. (2016) throughout the experiments reported. The team executed *in vitro* experiments, using Clone A HCV replicon cells and human primary hepatocytes to address the relevance of CatA and CES1 in the activation of the Sofosbuvir. Moreover, the team used siRNA mediated gene silencing, and Huh-7 cells. The aim of the latter experiment was to confirm the role of HINT1 in the metabolism of Sofosbuvir. Western blot analysis confirmed that only CatA was expressed in Clone A cells, and CatA and CES1 were expressed in primary human hepatocytes. These results suggest that the contribution of CatA and CES1 to the first step in Sofosbuvir metabolism is different in Clone A cells compared with primary human hepatocytes, although they both possess great relevance in the activation of Sofosbuvir (Murakami *et al.*, 2010). In addition to this, the team reported a 15-fold better hydrolyzation of Sofosbuvir by CatA compared to CES1. They also emphasized on the fact that, although CES1 had lower activity than CatA, its importance is prominent due to the protein's presence in hepatocytes (Murakami *et al.*, 2010).

6.3 Esterase in human plasma

When concerning drug metabolism, it is important to note that the drugs will be in direct contact with the recipient's blood. As there exist four different esterases in human plasma, it is worth considering that these might influence the hydrolysis of ester drugs or prodrugs (Li *et al.*, 2005). These four types are butyrylcholinesterase, paraoxonase, acetylcholinesterase, and albumin (Li *et al.*, 2005). However, carboxylesterase is not present in human plasma compared to various animals (Li *et al.*, 2005). In the studies by Murakami et al. (2010) and (2015) and by Birkus et al. (2016) the teams chose to study the activation of Sofosbuvir and Tenofovir in different cell lines or with recombinant enzymes. These *in vitro* experiments did not investigate what role plasma esterase might have on the ProTides. However, Murakami et al. (2015) did conduct an *in vivo* experiment concerning dogs where the plasma levels were reported (Murakami *et al.*, 2015). The reported levels suggest that both TAF and TDF might get metabolized in the plasma, as it was possible to determine the metabolite TVF (Murakami *et al.*, 2015). However, the team was also able to determine the liver levels of TFV, TFV-MP,

and TFV-DP, proving that drugs arrived at the liver and were not entirely metabolized by the plasma esterase (Murakami *et al.*, 2015).

In terms of Remdesivir, the ProTide is intravenously administrated and is initially in contact with plasma. It might be relevant to investigate how the esterases in human plasma respond to Remdesivir and if these causes too early activation of the ProTide. If this happens, the metabolite will not be able to penetrate the target cell and thereby not be able to stop the transcription of viral DNA. Pardo et al. (2020) investigated data from various articles containing information about Remdesivir's function. The article states that Remdesivir shows prominent effect when tested *in vitro* against Ebola, but also states that Remdesivir's effect in live subjects has proven disappointing (Pardo *et al.*, 2020). This information might support the idea that other esterases in the blood play a role in the early activation of Remdesivir. Furthermore, in the experiment by Murakami et al. (2015), the team also proved that it was possible to detect elevated TVF levels, which further supports that esterase in the blood might prematurely activate the prodrugs. However, how human plasma esterase effect ProTides activation – such as Remdesivir – still needs to be investigated, as this is not clearly understood.

According to Murakami et al. (2010), neutrophil elastase could cleave Sofobosvir *in vivo* (Murakami *et al.*, 2010). Neutrophils and macrophages secrete neutrophil elastase (Taylor *et al.*, 2018). The enzyme plays a critical role in immune response (Padmanabhan and Gonzalez, 2012) and is therefore present in a soluble state in the extracellular matrix and in plasma (Taylor *et al.*, 2018). This could suggest the involvement of neutrophil elastase in premature activation of intravenously administered ProTides, including Remdesivir. In order to confirm the relevance of neutrophil elastase in the metabolism of ProTides, experiments hereof is needed.

6.4 The proposed activation of Remdesivir

Based on the analysis of the three articles and the information regarding Tenofovir and Sofosbuvir, a proposed metabolism of Remdesivir will be presented and discussed. As all these substances are nucleotide analogs, it may be plausible to assume that all three ProTides share a similar mechanism to transform into their active state. Besides the authors' choice of method for the experiments, the conclusion was clear: CatA and CES1 play a role in the metabolism of Tenofovir and Sofosbuvir.

Presented below are the chemical structures of Tenofovir (and its prodrugs), Sofosbuvir, and Remdesivir. As mentioned in the section for Remdesivir, the drug is a C-adenosine nucleoside analog, meaning that the active compound mimics adenosine, used to elongate RNA and DNA monomers. Remdesivir has one phosphorous, which is masked by additional chemical groups, including phenyl and ester moieties. To achieve the pharmacologically active state of Remdesivir, the masking groups attached to the phosphorous, must be cleaved off.

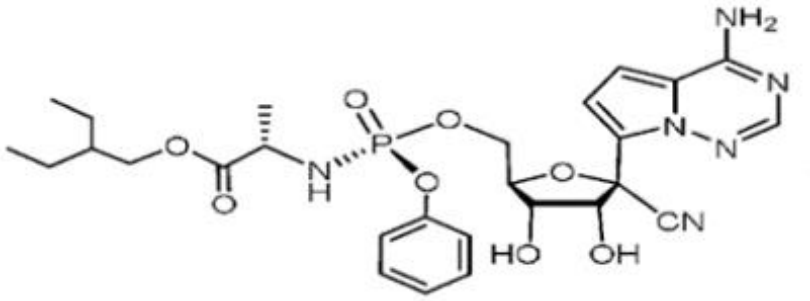

Figure 17: Chemical structure of Remdesivir (Jovanovic *et al.*, 2020).

This approach is a highly adopted method of the McGuigan type. The same approach is used to deliver antiviral effects of the drugs Tenofovir and Sofosbuvir. Tenofovir, and its prodrugs, are adenosine analogs (figure 18). The drugs share a similar structure to a certain extent. However, there is still significant structural difference between the compounds. Looking at the figures 17 and 18 both Remdesivir and Tenofovir, and their prodrugs, share the same purine structure. However, Remdesivir has one less nitrogen, and another is allocated. Compared to an adenosine purine, Tenofovir seem less modified.

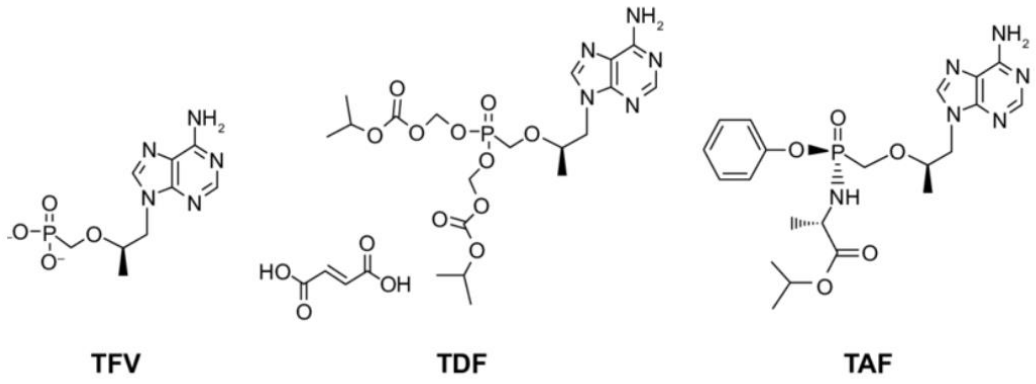

Figure 18: Chemical structure of Tenofovir and its prodrugs Tenofovir Disoproxil fumarate and Tenofovir Alafenamide (Ogawa, Furusyo and Nguyen, 2017)

Comparing Sofosbuvir and Remdesivir, they also share similarities, but not in terms of the analog. Sofosbuvir is composed of uracil (pyrimidine), which is structurally smaller than a purine as seen in figure 19. As Remdesivir, Sofosbuvir consists of a sugar-ring molecule. Notably, the sugar molecule is not present in TAF, making it an acyclic nucleotide analog.

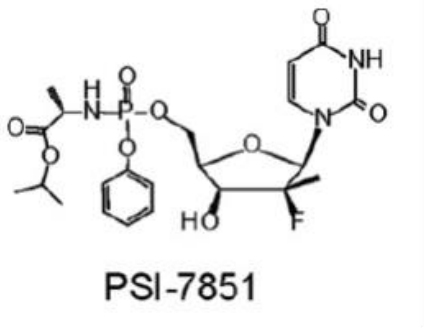

Figure 19: Chemical structrue of Sofosbuvir (PSI-7851) (Murakami et al., 2010).

Besides the analogs and sugar molecules, the 3 out of 4 groups on the phosphorous are very similar. Remdesivir and Sofosbuvir are both phosphoramidates, while Tenofovir is a phosphonamidate. As described in the section 1.6.2, the general structure includes an aryloxy triesterphosphramidate.

All three analyzed articles mention the ester's cleavage (R-CO-OR') was caused by CES1 and/or CatA. Based on the similar structure in Remdesivir, it might be possible that these enzymes can activate Remdesivir. Murakami et al. (2010), Birkus et al (2016), Murakami et al (2015) all reports pathways related to the studied ProTides which suggest the initial activation step in which CES1 is involved (Birkus *et al.*, 2016) (Murakami *et al.*, 2015). (Murakami *et al.*, 2010). It is important to emphasize the fact that all three studies concerning CES1 included hepatocytes. It can be discussed whether the enzymes involved in TAF and Sofosbuvir metabolism also apply to Remdesivir. Figure 20 illustrates a proposed metabolic pathway for Remdesivir, although no enzymes are reported to perform the first cleavage (Jovanovic *et al.*, 2020).

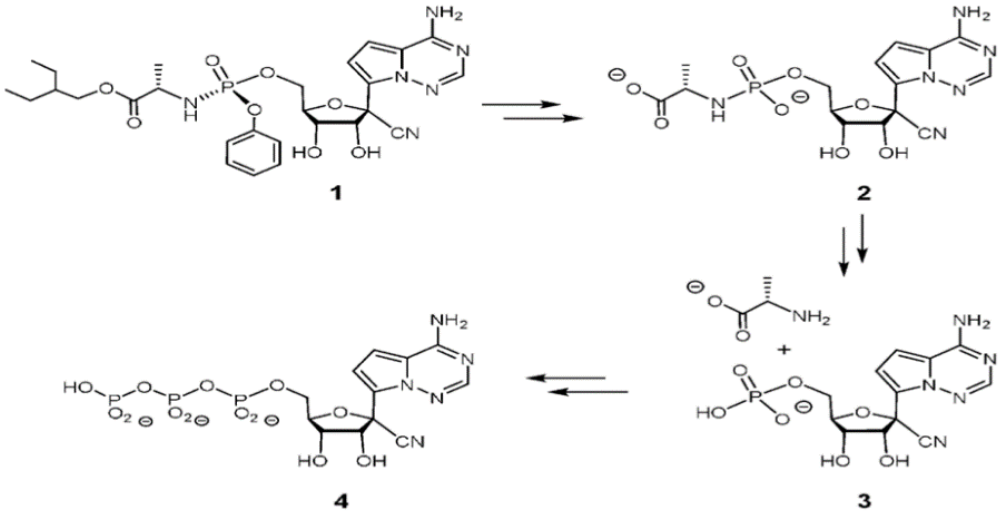

Figure 20: Proposed metabolic pathway of Remdesivir (Jovanovic *et al.*, 2020)

For each step, interacting enzymes continue to be unknown. However, by considering the first intermediates in Murakami et al. (2010), Birkus et al. (2016), and Murakami et al. (2015), the outcome is the same; the ester is cleaved, and a carboxylic acid terminal is produced. The intermediate for Remdesivir is equivalent, indicating the possibility of Remdesivir being cleaved by CES1 as probable. To further enhance the arguments, Remdesivir shows similar metabolism of the moieties as those proposed by Murakami et al. (2010), Birkus et al. (2016), and Murakami et al. (2015).

According to Murakami et al. (2010) and Murakami et al. (2015) HINT1 is involved in acid hydrolyzation, leading to an exposed monophosphate of the nucleotide analog (Murakami *et al.*, 2010). (Murakami *et al.*, 2015). According to Jovanovic et al. (2020) and Yan et al. (2020), HINT1 may subsequently cleave the first intermediate. Following the last step, the ProTides are phosphorylated to the active triphosphates (Murakami *et al.*, 2010). (Murakami *et al.*, 2015), (Birkus *et al.*, 2016), (Yan and Muller, 2020), (Jovanovic *et al.*, 2020). As the similarities for the activation of the ProTides are shown in more than one article, Remdesivir might eventually follow the same pathways. As ProTides serve the same purpose and have a similar structure, one might argue that the activation pathways share significant similarities and may include the same enzymes. Nonetheless, this analysis demonstrated that Remdesivir might be subject to hydrolyzation by CES1 in the initial activation step. However, mechanisms that activate Remdesivir in the human body is not fully understood. As Remdesivir is not used as a prodrug against liver diseases, it might be argued that it is unlikely that CES1 plays a significant role in the activation. Documented articles indicate that CatA is the major catalyzer outside the liver.

As Remdesivir might be susceptible to premature activation outside the cells, novel drug delivery methods could be considered. For instance, a study by Sahakijpijarn et al. (2020) suggested that Remdesivir can be produced as drug inhalation and might be used for lung-cell delivery (Sahakijpijarn *et al.*, 2020). The team concluded a delivery directly to the lungs in which Remdesivir appeared to be metabolized (Sahakijpijarn *et al.*, 2020). A delivery directly to the lungs might result in better outcomes in terms of viral infections in the lungs, such as those caused by SARS-CoV-2 (Sahakijpijarn *et al.*, 2020). Nonetheless, to further verify such claims, more research is needed.

7.0 Conclusion

According to various studies analyzed in this report, ProTides such as Sofosbuvir and Tenofovir can be metabolized by both CatA and CES1. Based on the information obtained in the articles, a proposed metabolism of Remdesivir was constructed. It was reported when considering the liver that CES1 might activate Remdesivir. However, CES1 is mostly abundant in liver tissue. The involvement of CES1 in other cells and tissues might not be as prominent. Therefore, it seems likely that CatA would activate Remdesivir if the target were in non-liver tissue. Furthermore, it was reported that HINT1 is involved in the acid hydrolyzation, which in turn resulted in exposed monophosphates of the nucleotide analogs. Evidence also suggests that HINT1 is involved in the cleavage of the first intermediate. The overall claim was that as the ProTides share a similar structure and function, they might also share a similar metabolic pathway. Laboratory experiments are needed to further investigate the metabolism of Remdesivir. This project demonstrates that expressing and purifying CES1 is a relatively cheap and a straightforward technique. Studies involving recombinant CES1, among other enzymes, and Remdesivir might be able to uncover the activation of the ProTide. However, an important point mentioned in this project was that esterase in blood might cause premature activation and that cell models do not illustrate the complicated nature of the human body. Therefore, a technique for delivery of the ProTide is of equal importance. A powder version of Remdesivir for inhalation was mentioned. It could be interesting to investigate Remdesivir's metabolism in lung cells compared to experimental procedures mentioned in the literary analysis.

Based on the experimental procedures it was possible to reproduce similar results reported in the article by Boonyuen et al. (2015). Purified protein was successfully tested for enzyme activity and the obtained K_m values were similar with the value in the article (570 µM and 580 µM compared to the reported value of 579 µM by Boonyuen et al. (2015)). This indicate that the article has reproducible procedures which may be used to future research in studies concerning metabolism initiated by CES1.

8.0 Future perspective

Although CES1 and CatA are the major enzymes responsible for the hydrolysis of antiviral drugs, further investigation is needed to understand the pathways in the human body. An approach for other studies could be a similar experiment as made in the project using recombinant CES1 and measuring enzyme activity. The aim would be to express the proteins in eukaryotic cells and thereby have a more complex environment, which can give a more dynamic picture of the enzyme's activity.

Moreover, the enzyme activity could be measured with other substrates suggesting other potential prodrugs hydrolyzed by CES1. ProTide technology is a powerful tool in drug discovery. Given its expanding applications, there is a real possibility that this technology will deliver new ProTides to treat various other diseases beyond viruses. A different approach would be to look at genetic variations of CES1 and see which effects it has on the activity of the enzyme. This would allow a better understanding of CES1 expression and activity and evolve personalized medicine to improve prodrugs' therapeutic outcomes.

9.0 Reference

1. Abet, V. *et al.* (2017) 'Prodrug approach: An overview of recent cases', *European Journal of Medicinal Chemistry*, 127, pp. 810–827. doi: 10.1016/j.ejmech.2016.10.061.
2. Agostini, M. L. *et al.* (2018) 'Coronavirus susceptibility to the antiviral remdesivir (GS-5734) is mediated by the viral polymerase and the proofreading exoribonuclease', *mBio*, 9(2), pp. 1–15. doi: 10.1128/mBio.00221-18.
3. Alanazi, A. S., James, E. and Mehellou, Y. (2019) 'The ProTide Prodrug Technology: Where Next?', *ACS Medicinal Chemistry Letters*, 10(1), pp. 2–5. doi: 10.1021/acsmedchemlett.8b00586.
4. Badgujar, K. C. *et al.* (2020) 'Remdesivir for COVID-19: A review of pharmacology, mechanism of action, in-vitro activity and clinical use based on available case studies', *Journal of Drug Delivery and Therapeutics*, 10(4-s), pp. 264–270. doi: 10.22270/jddt.v10i4-s.4313.
5. Birkus, G. *et al.* (2016) 'Intracellular activation of tenofovir alafenamide and the effect of viral and host protease inhibitors', *Antimicrobial Agents and Chemotherapy*, 60(1), pp. 316–322. doi: 10.1128/AAC.01834-15.
6. Bjerre, D. and Berg Rasmussen, H. (2018) 'Novel approach for CES1 genotyping: Integrating single nucleotide variants and structural variation', *Pharmacogenomics*, 19(4), pp. 349–359. doi: 10.2217/pgs-2016-0145.
7. Boonyuen, U. (2014) 'Human liver carboxylesterase 1 structure, polymorphism and its role in drug and prodrug activation and metabolism', *Journal of Medicine and Health Sciences*, pp. 11–24.
8. Boonyuen, U. *et al.* (2015) 'Efficient in vitro refolding and functional characterization of recombinant human liver carboxylesterase (CES1) expressed in E. coli', *Protein Expression and Purification*, 107, pp. 68–75. doi: 10.1016/j.pep.2014.11.006.
9. Cox, M. M., Doudna, J. A. and O'Donnell, M. (2015) *Molecular Biology – Principles and Practice*. second edition. W. H. Freeman and Company.
10. Doghaither, H. Al and Gull, M. (2010) 'Plasmids as Genetic Tools and Their Applications in Ecology and Evolution', *IntechOpen*, 524, pp. 141–157. doi: 10.5772/intechopen.85705.
11. Griffiths, A. J. F. *et al.* (2012) *Introduction to Genetic Analysis*. Tenth Edit. Edited by S. Winslow. New York: Palgrave macmillan.
12. Hiraiwa, M. (1999) 'Cathepsin A/protective protein: An unusual lysosomal multifunctional protein', *Cellular and Molecular Life Sciences*, 56(11–12), pp. 894–907. doi: 10.1007/s000180050482.
13. Holmes, R. S. *et al.* (2008) 'Opossum carboxylesterases: Sequences, phylogeny and evidence for CES gene duplication events predating the marsupial-eutherian common ancestor', *BMC*

Evolutionary Biology, 8(1), pp. 1–13. doi: 10.1186/1471-2148-8-54.

14. Hosokawa, M. (2008) 'Structure and catalytic properties of carboxylesterase isozymes involved in metabolic activation of prodrugs', *Molecules*, 13(2), pp. 412–431. doi: 10.3390/molecules13020412.
15. Huang, X. *et al.* (2016) 'Use of an improved matching algorithm to select scaffolds for enzyme design based on a complex active site model', *PLoS ONE*, 11(5), pp. 1–25. doi: 10.1371/journal.pone.0156559.
16. Imai, T. and Ohura, K. (2011) 'The Role of Intestinal Carboxylesterase in the Oral Absorption of Prodrugs', *Current Drug Metabolism*, 11(9), pp. 793–805. doi: 10.2174/138920010794328904.
17. Jovanovic, D. *et al.* (2020) 'The Enzyme-Free Release of Nucleotides from Phosphoramidates Depends Strongly on the Amino Acid'. doi: doi.org/10.1002/anie.202008665.
18. Li, B. *et al.* (2005) 'Butyrylcholinesterase, paraoxonase, and albumin esterase, but not carboxylesterase, are present in human plasma', *Biochemical Pharmacology*, 70(11), pp. 1673–1684. doi: 10.1016/j.bcp.2005.09.002.
19. Lodish, H., Berk, A. and Zipursky, S. (no date) *Molecular Cell Biology*. 4th editio. New York: W. H. Freeman. Available at: https://www.ncbi.nlm.nih.gov/books/NBK21498/.
20. Mahmoud, S. *et al.* (2018) 'Antiviral Nucleoside and Nucleotide Analogs: A Review', *Journal of Advanced Pharmacy Research*, 2(2), pp. 73–88. doi: 10.21608/aprh.2018.5829.
21. McMurry, J. *et al.* (2007) *Fundamentals of General, Organic, and Biological Chemistry*. sixth edit. Edited by N. Folchetti. Pearson Education, Inc.
22. Mehellou, Y., Balzarini, J. and McGuigan, C. (2009) 'Aryloxy phosphoramidate triesters: A technology for delivering monophosphorylated nucleosides and sugars into cells', *ChemMedChem*, 4(11), pp. 1779–1791. doi: 10.1002/cmdc.200900289.
23. Mehellou, Y., Rattan, H. S. and Balzarini, J. (2018) 'The ProTide Prodrug Technology: From the Concept to the Clinic', *Journal of Medicinal Chemistry*, 61(6), pp. 2211–2226. doi: 10.1021/acs.jmedchem.7b00734.
24. Minarowska, A. *et al.* (2012) 'Role of cathepsin A and cathepsin C in the regulation of glycosidase activity', *Folia Histochemica et Cytobiologica*, 50(1), pp. 20–24. doi: 10.5603/FHC.2012.0003.
25. Moran, L. A. *et al.* (2014) *Principles of Biochemistry*. Fifth. Pearson Education Limited.
26. Murakami, E. *et al.* (2010) 'Mechanism of activation of PSI-7851 and its diastereoisomer PSI-7977', *Journal of Biological Chemistry*, 285(45), pp. 34337–34347. doi: 10.1074/jbc.M110.161802.
27. Murakami, E. *et al.* (2015) 'Implications of efficient hepatic delivery by tenofovir alafenamide (GS-7340) for hepatitis B virus therapy', *Antimicrobial Agents and Chemotherapy*, 59(6), pp. 3563–3569. doi: 10.1128/AAC.00128-15.

28. Murphy, B. G. *et al.* (2018) 'The nucleoside analog GS-441524 strongly inhibits feline infectious peritonitis (FIP) virus in tissue culture and experimental cat infection studies', *Veterinary Microbiology*, 219(April), pp. 226–233. doi: 10.1016/j.vetmic.2018.04.026.
29. Nzabonimpa, G. S. *et al.* (2016) 'Investigating the impact of missense mutations in hCES1 by in silico structure-based approaches', *Drug Metabolism and Personalized Therapy*, 31(2), pp. 97–106. doi: 10.1515/dmpt-2015-0034.
30. Ogawa, E., Furusyo, N. and Nguyen, M. H. (2017) 'Tenofovir alafenamide in the treatment of chronic hepatitis B: Design, development, and place in therapy', *Drug Design, Development and Therapy*, 11, pp. 3197–3204. doi: 10.2147/DDDT.S126742.
31. Padmanabhan, J. and Gonzalez, A. L. (2012) 'The Effects of Extracellular Matrix Proteins on Neutrophil-Endothelial Interaction - A Roadway To Multiple Therapeutic Opportunities', *Yale Journal of Biology and Medicine*, 85(2), pp. 167–185.
32. Pardo, J. *et al.* (2020) 'The journey of remdesivir: From Ebola to COVID-19', *Drugs in Context*, 9, pp. 1–9. doi: 10.7573/DIC.2020-4-14.
33. Rasmussen, H. B. *et al.* (2015) 'Pharmacogenomics Individualization of treatments with drugs'.
34. Reza Hashemian, S. M., Farhadi, T. and Velayati, A. A. (2020) 'A review on remdesivir: A possible promising agent for the treatment of COVID-19', *Drug Design, Development and Therapy*, 14, pp. 3215–3222. doi: 10.2147/DDDT.S261154.
35. Van Rompay, A. R., Johansson, M. and Karlsson, A. (2003) 'Substrate specificity and phosphorylation of antiviral and anticancer nucleoside analogues by human deoxyribonucleoside kinases and ribonucleoside kinases', *Pharmacology and Therapeutics*, 100(2), pp. 119–139. doi: 10.1016/j.pharmthera.2003.07.001.
36. Sahakijpijarn, S. *et al.* (2020) 'Development of remdesivir as a dry powder for inhalation by thin film freezing', *Pharmaceutics*, 12(11), pp. 1–27. doi: 10.3390/pharmaceutics12111002.
37. Schreuder, H. A. *et al.* (2014) 'Crystal structure of cathepsin A, a novel target for the treatment of cardiovascular diseases', *Biochemical and Biophysical Research Communications*, 445(2), pp. 451–456. doi: 10.1016/j.bbrc.2014.02.014.
38. Siegel, D. *et al.* (2017) 'Discovery and Synthesis of a Phosphoramidate Prodrug of a Pyrrolo[2,1-f][triazin-4-amino] Adenine C-Nucleoside (GS-5734) for the Treatment of Ebola and Emerging Viruses', *Journal of Medicinal Chemistry*, 60(5), pp. 1648–1661. doi: 10.1021/acs.jmedchem.6b01594.
39. Slusarczyk, M., Serpi, M. and Pertusati, F. (2018) *Phosphoramidates and phosphonamidates (ProTides) with antiviral activity, Antiviral Chemistry and Chemotherapy*. doi: 10.1177/2040206618775243.
40. Taylor, S. *et al.* (2018) 'The role of neutrophils and neutrophil elastase in pulmonary arterial hypertension', *Frontiers in Medicine*, 5(AUG), pp. 1–1. doi: 10.3389/fmed.2018.00217.

41. Wang, D. *et al.* (2018) 'Human carboxylesterases: a comprehensive review', *Acta Pharmaceutica Sinica B*, 8(5), pp. 699–712. doi: 10.1016/j.apsb.2018.05.005.
42. Wiemer, A. J. and Wiemer, D. F. (2014) 'Prodrugs of Phosphonates and Phosphates: Crossing the Membrane Barrier', *Springer International*, pp. 115–160. doi: 10.1007/128_2014_561.
43. Yan, V. C. and Muller, F. L. (2020) 'Advantages of the Parent Nucleoside GS-441524 over Remdesivir for Covid-19 Treatment'.
44. Zhu, W. *et al.* (2020) 'RNA-Dependent RNA Polymerase as a Target for COVID-19 Drug Discovery', *SLAS Discovery*, 25(10), pp. 1141–1151. doi: 10.1177/2472555220942123.